



# Determination of the structure of disordered overlayers of ethylene on clean and hydrogen-covered Pd(111) by low-energy electron diffraction

T. Zheng<sup>a</sup>, D. Stacchiola<sup>a</sup>, H.C. Poon<sup>b</sup>, D.K. Saldin<sup>b</sup>, W.T. Tysoe<sup>a,\*</sup>

<sup>a</sup> *Laboratory for Surface Studies, Department of Chemistry and Biochemistry, University of Wisconsin–Milwaukee, Milwaukee WI 53211, USA*

<sup>b</sup> *Laboratory for Surface Studies, Department of Physics, University of Wisconsin–Milwaukee, Milwaukee WI 53211, USA*

Received 16 February 2004; accepted for publication 3 June 2004

Available online 19 June 2004

## Abstract

The surface structure of the disordered overlayer formed by ethylene adsorption on Pd(111) at 80 K is determined by low-energy electron diffraction (LEED) from the effects of chemisorbed molecules on the intensity versus beam energy ( $I/E$ ) variation of the substrate ( $1 \times 1$ ) Bragg spots. It is shown that ethylene is di- $\sigma$ -bonded on clean Pd(111), where the measured geometry is in agreement with the results of previous density functional theory (DFT) calculations. The structure of a disordered overlayer of ethylene on hydrogen-covered Pd(111) at 80 K is also measured using LEED and is found to form a  $\pi$ -bonded species in accord with previous infrared results.

© 2004 Elsevier B.V. All rights reserved.

**Keywords:** Low energy electron diffraction (LEED); Surface structure, morphology, roughness, and topography; Chemisorption; Palladium; Alkenes

## 1. Introduction

The surface chemistry of ethylene has been extensively studied on late transition-metal surfaces since these are generally active ethylene hydrogenation catalysts [1]. This reaction on palladium is of special interest since it provides the basis for a particularly selective catalyst for the production of polymer-grade ethylene, allowing

small concentrations of acetylene in ethylene feedstocks to be selectively hydrogenated to ethylene, without ethylene hydrogenation to ethane [2–5]. It has been found that ethylene adsorbs in a di- $\sigma$  configuration on clean Pd(111) [6–8], but converts to  $\pi$ -bonded species on a hydrogen-covered surface [6]. The  $\pi$ -bonded species, being more weakly adsorbed, are proposed to react preferentially with hydrogen to form ethane [9–13]. It has been demonstrated that subsurface rather than surface hydrogen is responsible for the rehybridization of ethylene on Pd(111) at low temperatures [14]. Unfortunately, there is a paucity of structural measurements of ethylene adsorbed on

\* Corresponding author. Tel.: +414-229-5222; fax: +414-229-5036.

E-mail address: [wtt@uwm.edu](mailto:wtt@uwm.edu) (W.T. Tysoe).

transition-metal surfaces, primarily since it does not form ordered overlayers and is therefore not amenable to standard LEED intensity versus energy ( $I/E$ ) structural analyses. An effort has been made to overcome this problem by using the diffuse background scattering in LEED to measure the structure of ethylene on Pt(111) [15]. An arrangement of tilted ethylene species, adsorbed on face-centered-cubic (fcc) and hexagonal-close-packed (hcp) sites was proposed on Pt(111) at a temperature of 200 K [15]. Since the diffuse background scattering is very weak, however, such measurements are extremely difficult. Held and Steinrück [16] have proposed the analysis of the intensities of the specular LEED spot to overcome this problem. We have recently demonstrated that the effect on all the substrate ( $1 \times 1$ ) Bragg spots due to the presence of an adsorbed layer is approximately two orders of magnitude larger than the diffuse scattering [17]. This increased intensity makes it much easier to collect diffraction data from disordered overlayers. Use of the intensities of several Bragg spots facilitates the determination of the structures of such systems. This idea has been previously exploited by Gautier et al. [18] to examine the surface composition and structure of disordered alloys, and by Schwennicke et al. [19] and Seitsonen et al. [20] to study disordered adsorbates on surfaces. The LEED calculations were performed for (relatively large) overlayer unit cells of the same coverage,  $\Theta$ , as the disordered overlayer. We have pointed out in our recent study of a disordered overlayer of methanol on Pd(111) [17] that the  $I/E$  curves of the integer-order (or  $1 \times 1$ ) Bragg spots in such cases may be calculated to a very good approximation much more rapidly by assuming a  $1 \times 1$  overlayer of artificial molecules with a scattering factor reduced by a factor  $\Theta$ . The structure of acetylene [21] on Pd(111) was measured both from the overlayer and  $1 \times 1$  spots, where both methods yielded identical structures. In the following, this strategy is used to determine the structures of ethylene on clean and hydrogen-covered Pd(111) in order to correlate this information with their observed infrared spectra and to provide insights into the ethylene hydrogenation chemistry on Pd(111).

## 2. Experimental

LEED measurements were carried out in a doubly  $\mu$ -metal shielded, ultrahigh vacuum chamber operating at a base pressure of  $\sim 5 \times 10^{-11}$  Torr. The experimental method has been previously described in detail [17]. Briefly, the LEED patterns of the surface were photographed as a function of incident energy using a Nikon Coolpix digital camera (5.0 MPixel resolution) and the images stored on an IBM Smartcard memory (1 Gbytes). The images were then downloaded to a personal computer for subsequent analysis where the  $I/E$  curves were generated by measuring the intensity of the diffraction spots using NIHImage [22].

The Pd(111) single crystal was cleaned using a standard protocol and its cleanliness monitored using Auger spectroscopy and temperature-programmed desorption collected following oxygen adsorption. The ethylene (Matheson, Research Grade) and hydrogen (Praxair, 99.9999%) were transferred to glass bottles, which were attached to the gas-handling line for introduction into the vacuum chamber.

## 3. Calculations

The  $I/E$  curves for the adsorbed layer were simulated from a standard LEED computer program by a calculation for an ordered overlayer of the smallest possible ( $1 \times 1$ ) periodicity with fractional occupancy of the same magnitude as the coverage  $\Theta$ . The notion that a calculation involving only integer-order beams may be sufficiently accurate for practical calculations of the integer-order Bragg spots for large unit-cell overlayers may be regarded as a special case of the beam set neglect method [23]. The extra simplification introduced in the present paper is that the quasidynamical treatment [24] of the adlayer allows it to be treated as literally a  $1 \times 1$  overlayer with an adsorbate scattering factor of each of the constituent atoms reduced by a factor of  $\Theta$ . For a nearly flat-lying carbon-carbon bond, which is the case for the molecules studied here, this reduces the molecular scattering factor by the same amount  $\Theta$  within the quasidynamical approximation. Such

an analysis of the data of integer-order Bragg spots may be used to find the structures of both ordered and disordered adsorbates, as shown by a recent determination of the structures of disordered methanol ( $\text{CH}_3\text{OH}$ ) on Pd(111) [17] and ordered acetylene ( $\text{C}_2\text{H}_2$ ) on Pd(111) [21].

The general methodology of our calculations was the following: the angles of incidence of the electron beam for both the clean and adsorbate-covered surfaces were determined using a standard LEED package [25] to find the best fit of calculated  $I/E$  curves to the clean Pd(111) data. A constrained global search was then conducted for the adsorbate-covered surfaces with the bond length, inclination of the C–C axis and substrate atoms fixed. The approximate structural model obtained by the global search was used as a reference point for structural refinement, which allows for variations of substrate atom positions using automated tensor LEED [26].

## 4. Results and discussion

### 4.1. Structure of ethylene on clean Pd(111)

It has been shown previously that di- $\sigma$ -bonded species found at 80 K on the clean Pd(111) surface exhibit an infrared peak at  $1103\text{ cm}^{-1}$ , assigned to a  $\text{CH}_2$  wagging mode [6]. This vibrational frequency suggests that ethylene is rehybridized on the Pd(111) surface, but to a lesser extent than on Pt(111) [27] and Ni(111) [28], and to a greater extent than on Ru(001) [29]. The relative intensities of the features indicate that the ethylenic carbon–carbon axis lies parallel to the surface. No ordered LEED structures are observed for this species. The LEED  $I/E$  curves of the  $(1 \times 1)$  spots were collected for clean and ethylene-covered surfaces (following a 2.5 L exposure,  $1\text{ L} = 1 \times 10^{-6}$  Torr). Note that exposures are not corrected for ionization gauge sensitivities. Based on molecular beam experiments, this exposure leads to a coverage of  $\sim 0.25$  monolayers (where a monolayer is defined relative to the Pd atom density on the (111) surface). A coverage lower than saturation was selected to avoid possible complications due to second-layer adsorption [6]. Typical experimental

LEED  $I/E$  curves for six  $(1 \times 1)$  beams are shown in Fig. 1 (solid line), which plot the spot intensities in arbitrary units versus the beam energy. In view of the infrared results, the carbon–carbon bond of ethylene was constrained to be parallel to the surface and the carbon–carbon bond length fixed at  $1.45\text{ \AA}$ , almost midway between the double bond length of  $1.35\text{ \AA}$  and the single bond length of  $1.54\text{ \AA}$  [30]. This value will be allowed to relax in a final tensor-LEED refinement. In addition, the palladium–palladium distances were fixed at their bulk palladium value of  $2.75\text{ \AA}$  [30]. The vertical distance of the adsorbed ethylene molecule to the Pd(111) surface was allowed to vary between  $1.7$  and  $2.1\text{ \AA}$  in steps of  $0.1\text{ \AA}$ , and the azimuthal rotation angle of the carbon–carbon bond around a normal to the surface was varied in steps of  $30^\circ$ . A global structural search was carried out to find the minimum Pendry  $R$ -factor [31] over the range of heights and angles described above for one of the carbon atoms located at each of 21 points distributed throughout the reduced Wigner–Seitz cell (indicated in Fig. 2). The resulting contour map of the Pendry  $R$ -factor of one of the carbon atoms (designated  $\text{C}_1$ ) within the reduced Wigner–Seitz cell, for the height of the molecule above the surface ( $1.9\text{ \AA}$ ) and the C–C azimuthal angle ( $0^\circ$ ) that yielded the lowest overall  $R$ -factor, is displayed in Fig. 2. Also marked on this figure are the positions of the atop, bridge and the two types of three-fold hollow sites as well as the position with the minimum Pendry  $R$ -factor. The value of  $\Delta R$  is  $\sim 0.02$  [31] for the total experimental energy range used in these experiments, indicating that the minimum value in the contour plot of Fig. 2 is statistically significant.

This geometry was then used as the input to a tensor LEED calculation. This was performed for various coverages of the flat-lying species and yielded the lowest  $R$ -factor value at 0.25 monolayers, in accord with the coverage expected from the ethylene exposure. The final result gave an  $R$ -factor of 0.31. The resulting structure is depicted in Fig. 3, where the hydrogen atoms, not determined by LEED, have been added for clarity, and the relevant coordinates summarized in Table 1. The LEED experiment and resulting structure determinations were carried out at least three

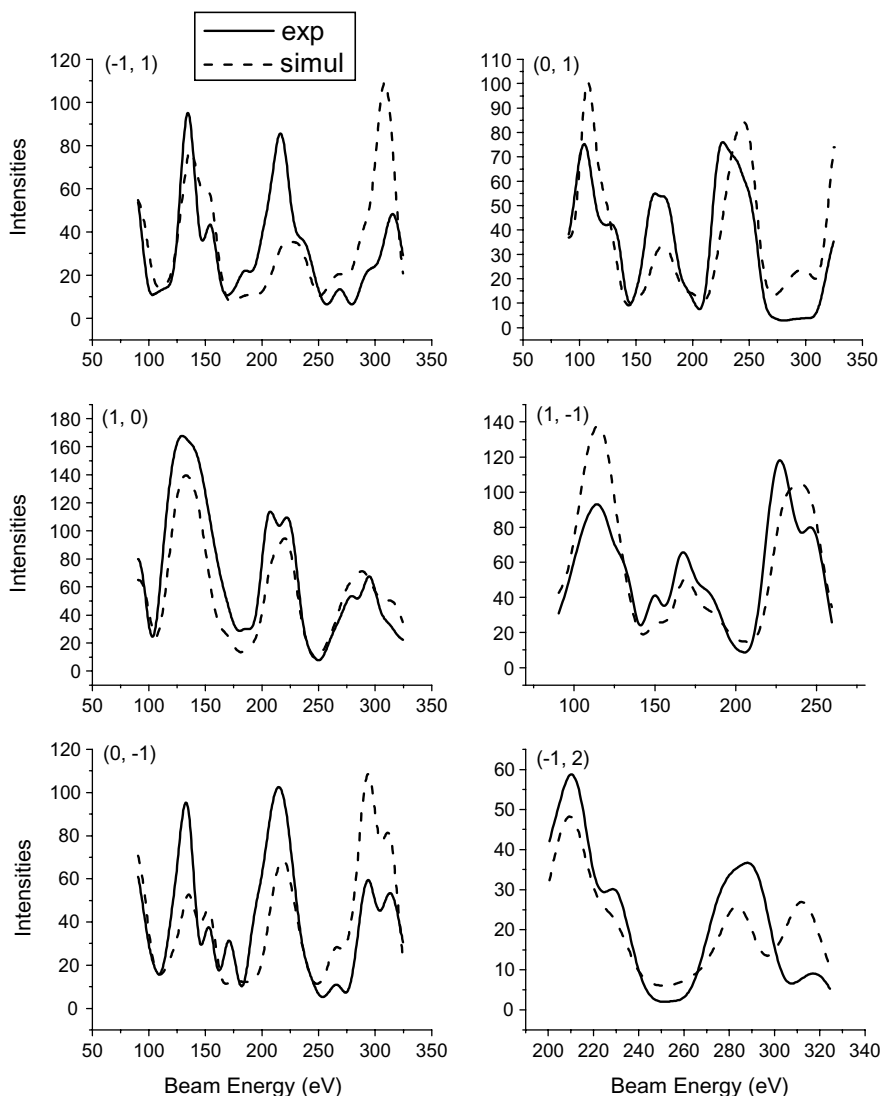


Fig. 1. Typical LEED  $I/E$  curves for ethylene (2.5 L) adsorbed on Pd(111) at 80 K (solid line). Shown for comparison are the calculated curves for the best-fit structures for a parallel ethylene structure (dotted lines, see text).

times. The error in the geometry shown in Table 1 was determined by measuring the change in  $R$ -factor as a function of each parameter and defining in the error in the parameter as that for which the  $R$ -factor changes by 0.02 [31]. The lowest  $R$ -factor for a parallel structure is for adsorption at a short-bridge site with a carbon–carbon bond length of  $1.42 \pm 0.09$  Å, in agreement with the value expected for a di- $\sigma$ -bonded

species. The geometry of this species is very close to that found from density functional theory (DFT) calculations [7,32], which also predict an ethylene species bonded across the short bridge on the surface with a carbon–carbon bond length of 1.45 Å and a palladium–carbon distance of 2.19 Å, although the latter value is somewhat longer than the value measured from LEED ( $1.96 \pm 0.05$  Å).

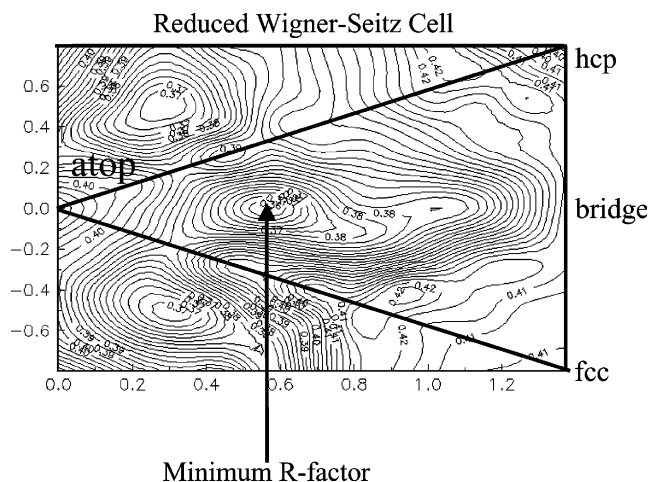


Fig. 2. Typical contour map of the Pendry  $R$ -factor for ethylene adsorbed on Pd(111) at 80 K as a function of position of one of the carbon atoms (designated  $C_1$ ) within the reduced Wigner–Seitz cell, with the ethylenic carbon–carbon bond constrained to be parallel to the surface and fixed at 1.45 Å. The vertical distance of the molecule to the surface is varied from 1.7 to 2.1 Å in steps of 0.1 and the molecule allowed to rotate azimuthally in steps of 30°.

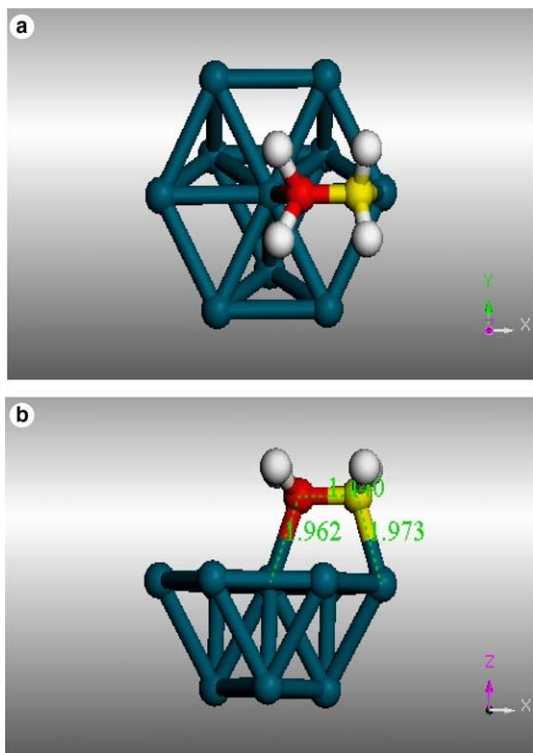


Fig. 3. Schematic depiction of the structure of di- $\sigma$ -bonded ethylene formed at 80 K on Pd(111): (a) top view and (b) side view.

In previous analyses of the diffuse LEED pattern for ethylene on Pt(111), two tilted structures were found; one located above the hcp site with the C–C axis tilted at  $\sim 20^\circ$ , and a second species also with the C–C axis tilted at  $\sim 20^\circ$  with respect to the surface located above the fcc site [15]. In view of this, a global search was carried out, similar to that done for the parallel species above, but now with the carbon–carbon bond tilted with respect to the surface by  $20^\circ$ . A contour plot of Pendry  $R$ -factors within the reduced Wigner–Seitz cell was constructed in a similar manner as described above, where now the minimum indicates that  $C_1$  is located close to the hcp three-fold hollow site, with a similar Pendry  $R$ -factor as found for the di- $\sigma$ -bonded species above. A tensor LEED calculation was then performed for a surface comprising a mixture of both the parallel (di- $\sigma$ -bonded) and tilted species with various proportions of each. The Pendry  $R$ -factor was plotted as a function of the proportion of the tilted species (the remainder being di- $\sigma$ -bonded ethylene), which yielded a minimum at about 15% tilted species. However, the change in the value of the Pendry  $R$ -factor as a function of proportion of the tilted species was  $\sim 0.02$ , within the precision of the  $R$ -factor [31] so that no definitive conclusion can be arrived at

Table 1

Measured distances for di- $\sigma$ -bonded ethylene on clean Pd(111) at 80 K from an analysis of the LEED  $I/E$  curves compared with the calculated structure for di- $\sigma$ -bonded ethylene on Pd(111)

	80 K	DFT calculation [7,32]
$d(\text{C}-\text{C})/\text{\AA}$	$1.42 \pm 0.09$	1.45
$d(\text{C}_1-\text{Pd})/\text{\AA}$	$1.96 \pm 0.05$	2.19
$d(\text{C}_2-\text{Pd})/\text{\AA}$	$1.96 \pm 0.05$	2.19
$d_z(\text{C}-\text{Pd})/\text{\AA}$	$1.85 \pm 0.05$	2.10
$\theta_{\text{tilt}}(\text{C}-\text{C})/^\circ$	$2 \pm 4$	0

concerning the presence of a tilted species. Further experiments will be carried out using a larger energy range to attempt to unequivocally identify the presence of a co-adsorbed, tilted ethylenic species.

#### 4.2. Structure of ethylene on hydrogen-covered Pd(111)

Previous RAIRS studies of ethylene on hydrogen-covered Pd(111) reveal that the presence of sub-surface hydrogen causes di- $\sigma$ -bonded ethylene to convert into a more weakly adsorbed,  $\pi$ -bonded species [6,14]. It has been shown that the relative proportions of  $\pi$ - and di- $\sigma$ -bonded species vary linearly with hydrogen coverage. It was further demonstrated, by taking advantage of the fact that the ratio of surface and subsurface hydrogen depends on the temperature [33,34], that the formation of  $\pi$ -bonded ethylene was induced by the presence of sub-surface hydrogen [14].

LEED  $I/E$  curves were measured with the sample held at 80 K after the surface had been pre-dosed with 10 L of hydrogen to form a saturated overlayer, and then exposed to 2.5 L of ethylene. The resulting data were analyzed in a similar manner as for di- $\sigma$ -bonded ethylene; a global structural search was carried out with ethylene lying parallel to the surface, the bond length fixed at 1.40  $\text{\AA}$ , and the palladium–palladium distance fixed at the bulk value (2.75  $\text{\AA}$ ). The position of one of the carbon atoms was varied over 21 points within the reduced Wigner–Seitz cell, the vertical distance from the ethylenic carbon atoms to the palladium surface varied between 1.9 and 2.3  $\text{\AA}$  in steps of 0.1  $\text{\AA}$ , and the azimuthal C=C angle varied in steps of 30°. The resulting structural

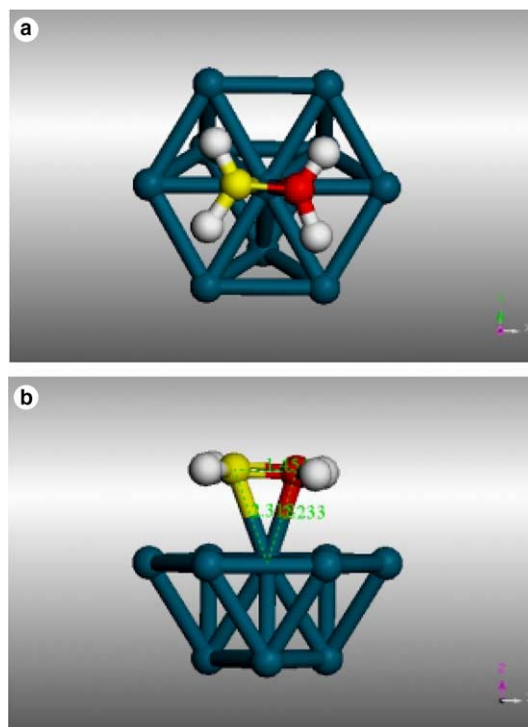


Fig. 4. Depiction of the structure of  $\pi$ -bonded ethylene formed at 80 K on hydrogen-covered Pd(111): (a) top view and (b) side view.

parameters were used as an input to the tensor LEED program. Note that this program allows both the palladium and carbon atoms to relax and yielded an  $R$ -factor of 0.31 for the best structure. The resulting geometry is displayed in Fig. 4, where again the hydrogen atoms have been added for clarity. This reveals that ethylene now adsorbs over an atop site with the C=C axis essentially parallel to a vector joining nearest-neighbor palladium atoms on the (111) surface, and the resulting structural parameters are shown in Table 2. This reveals a slight tilt (of  $2^\circ \pm 4^\circ$ ), within the precision of the measurement and indicates that the C=C bond is essentially parallel to the surface. The bond length is  $1.45 \pm 0.10$   $\text{\AA}$ , where again the error is estimated using the method suggested by Pendry [31], and is approximately the same as found for di- $\sigma$ -bonded ethylene. However, the accuracy of distances parallel to the surface measured by LEED is not high. The structure of

Table 2

Calculated distances for  $\pi$ -bonded ethylene on hydrogen-covered Pd(111) at 80 K from an analysis of the LEED  $I/E$  curves compared with the calculated structure for  $\pi$ -bonded ethylene

	80 K	DFT calculation [7,32]
$d(\text{C}-\text{C})/\text{\AA}$	$1.45 \pm 0.10$	1.40
$d(\text{C}_1-\text{Pd})/\text{\AA}$	$2.28 \pm 0.12$	2.24
$d(\text{C}_2-\text{Pd})/\text{\AA}$	$2.28 \pm 0.12$	2.24
$d_z(\text{C}-\text{Pd})/\text{\AA}$	$2.17 \pm 0.12$	2.13
$\theta_{\text{tilt}}(\text{C}-\text{C})/^\circ$	$2 \pm 4$	0

$\pi$ -bonded ethylene has been calculated on Pd(111) using DFT [7,32] and predicts ethylene adsorption on an atop site with the carbon–carbon axis oriented as shown in Fig. 4. The calculated carbon–carbon bond length is 1.395 Å, in satisfactory agreement with the measured value (Table 2) and the calculated carbon–palladium distance is 2.24 Å, in excellent agreement with the value measured by LEED ( $2.28 \pm 0.12$  Å). DFT calculations further suggest that the  $\pi$ -bonded species interacts only weakly with the surface primarily through van der Waals interactions with a heat of adsorption of  $\sim 27$ – $30$  kJ/mol. Temperature-programmed desorption data show that ethylene desorbs from hydrogen-saturated Pd(111) at  $\sim 220$  K [35].

## 5. Conclusions

LEED determinations of the structure of ethylene on Pd(111) at 80 K show the presence of both di- $\sigma$ -bonded ethylene. LEED also confirms that ethylene forms a  $\pi$ -bonded species on hydrogen-covered Pd(111). The structures of  $\pi$ - and di- $\sigma$ -bonded ethylene and the vinyl species are all in good agreement with the results of DFT calculations.

## Acknowledgements

WTT gratefully acknowledges support of this work by the US Department of Energy (DOE), Division of Chemical Sciences, Office of Basic Energy Sciences, under grant number DE-FG02-92ER14289, and DKS the DOE Division of

Materials Science and Engineering, for grant number DE-FG02-84ER45076.

## References

- [1] G.C. Bond, P.B. Wells, *Adv. Catal.* 15 (1964) 91.
- [2] A.N.R. Bos, K.R. Westerterp, *Chem. Eng. Proc.* 32 (1993) 1.
- [3] A. Borodzinski, A. Golebiowski, *Langmuir* 13 (1997) 883.
- [4] P.A. Sheth, M. Neurock, C.M. Smith, *J. Phys. Chem. B.* 107 (2003) 2009.
- [5] J. Gislason, W. Xia, H. Sellars, *J. Phys. Chem. A.* 106 (2002) 767.
- [6] D. Stacchiola, L. Burkholder, W.T. Tysoe, *Surf. Sci.* 511 (2002) 215.
- [7] M. Neurock, R.A. Van Santen, *J. Phys. Chem. B.* 105 (2000) 11127.
- [8] M. Sock, A. Eichler, S. Surnev, J.N. Andersen, B. Klotzer, K. Hayek, M.G. Ramsey, F.P. Netzer, *Surf. Sci.* 545 (2003) 122.
- [9] P.S. Cremer, X. Su, R. Shen, G.A. Somorjai, *J. Am. Chem. Soc.* 118 (1996) 2942.
- [10] D. Stacchiola, S. Azad, L. Burkholder, W.T. Tysoe, *J. Phys. Chem. B.* 105 (2001) 11233.
- [11] Sh. Shaikhutdinov, M. Heemeier, M. Bäumer, T. Lear, D. Lennon, R.J. Oldman, S.D. Jackson, H.J. Freund, *J. Catal.* 200 (2001) 330.
- [12] Sh. Shaikhutdinov, M. Frank, M. Bäumer, S.D. Jackson, R.J. Oldman, J.C. Hemminger, H.J. Freund, *Catal. Lett.* 80 (2002) 115.
- [13] H. Ofner, F. Zaera, *J. Am. Chem. Soc.* 124 (2002) 10982.
- [14] D. Stacchiola, W.T. Tysoe, *Surf. Sci.* 540 (2003) L600.
- [15] R. Döll, C.A. Gerken, M.A. Van Hove, G.A. Somorjai, *Surf. Sci.* 374 (1997) 151.
- [16] G. Held, H.-P. Steinrück, *Surf. Sci.* 490 (2001) 274.
- [17] H.C. Poon, M. Weinert, D.K. Saldin, D. Stacchiola, T. Zheng, W.T. Tysoe, *Phys. Rev. B.* 69 (2004) 035401.
- [18] Y. Gauthier, Y. Joly, R. Baudoing, J. Rundgren, *Phys. Rev. B.* 31 (1985) 6216.
- [19] C. Schwennicke, C. Voges, H. Pfnür, *Surf. Sci.* 349 (1996) 185.
- [20] A.P. Seitsonen, Y.D. Kim, M. Krapp, S. Wendt, H. Over, *Phys. Rev. B.* 65 (2001) 035413.
- [21] T. Zheng, W.T. Tysoe, H.C. Poon, D.K. Saldin, *Surf. Sci.* 543 (2003) 19.
- [22] NIH Image is available from <http://rsb.info.nih.gov/nib-image/>.
- [23] M.A. Van Hove, R. Lin, G.A. Somorjai, *Phys. Rev. Lett.* 51 (1983) 778.
- [24] N. Bickel, K. Heinz, *Surf. Sci.* 163 (1985) 435.
- [25] M.A. Van Hove, S.Y. Tong, *Surface Crystallography by LEED*, Springer, Heidelberg, 1977.
- [26] A. Barbieri, P.J. Rous, A. Wander, M.A. Van Hove, Automated Tensor LEED Programs package, available from M.A. Van Hove.

- [27] J. Fan, M. Trenary, *Langmuir* 10 (1994) 3649.
- [28] E. Cooper, R. Raval, *Surf. Sci.* 333 (1995) 94.
- [29] P.M. Parlett, M. Chesters, *Surf. Sci.* 358 (1996) 791.
- [30] R.C. Weast (Ed.), *CRC Handbook of Physics and Chemistry*, CRC Press, Boca Raton, FL, 1988.
- [31] J.B. Pendry, *J. Phys. C* 13 (1980) 937.
- [32] Q. Ge, M. Neurock, *Chem. Phys. Lett.* 358 (2002) 377.
- [33] M.S. Daw, S.M. Foiles, *Phys. Rev. B.* 35 (1987) 2128.
- [34] T.E. Felter, E.C. Sowa, M.A. Van Hove, *Phys. Rev. B.* 40 (1989) 891.
- [35] L. Burkholder, D. Stacchiola, W.T. Tysse, *Surf. Rev. Letts.* 10 (2003) 909.